Measurement 46 (2013) 2093–2098

Contents lists available at SciVerse ScienceDirect

Measurement

journal homepage: www.elsevier.com/locate/measurement

Perception of effective contact area distribution for humanoid robot foot

Baoyuan Wu [a,*], Zengfu Wang [a], Jianfei Luo [b], Zhongcheng Wu [b]

[a] Institute of Intelligent Machines, Chinese Academy of Sciences, Hefei 230031, China
[b] High Magnetic Field Laboratory, Chinese Academy of Sciences, Hefei 230031, China

ARTICLE INFO

Article history:
Received 5 June 2012
Received in revised form 21 March 2013
Accepted 26 March 2013
Available online 10 April 2013

Keywords:
Humanoid robot
Flexible force sensor array (FFSA)
Effective contact area (ECA)
ZMP

ABSTRACT

Maintaining dynamical stability for humanoid robots to walk or run in even environments has so far been achieved. However, it will become a challenge work to keep balance under rough terrains, because the effective contact area (ECA) between the feet and the uneven environments is less than that on even ground. Thus some control schemes are additionally needed for robot to keep dynamical balance, which increases the complexity of control. In view of that, flexible force sensor array (FFSA) system is adopted under robot feet to detect the ECA in the case of stepping on rough terrains. Structure optimum, data acquisition, processing methods, etc., of the FFSA system are all elaborately provided in this paper. And the feasibility and validity of the FFSA system mounted in the robot foot system are experimentally tested on the humanoid robot platform BHR-2.

1. Introduction

The realization for humanoid robots to walk or run dynamically and stably on various kinds of rough terrains has long been considered as the research emphases. Unlike multi-legged robots that can benefit from a stable base of three or more contact regions, the humanoid robot is forced to maintain stability with only one or two contact regions [1–3]. The foot system constitutes the element which ensures the interaction between the humanoid robot and the environment. Apart from supporting the whole weight of robot and sensing external forces, perception of effective contact area (ECA) of foot on rough terrains is indispensably important information supports for various control schemes. A dynamic equilibrium criterion – Zero Moment Point (ZMP) has so far been extensively employed in humanoid robot control [4–7]. Most stable motion control algorithm bases on the assumption that the actual ZMP is always in the support polygon area formed by the contour of the robot feet during walking [8–9]. However, it is not suitable for balance control especially in the case of stepping on rough terrains. And it is difficult to keep ZMP in the small support polygon even though the robot is controlled by a moment compensatory method.

The humanoid robots ASIMO [10], HRP-2 [11], HUBO [12], etc. had also rubber layer set under soles plate for impact absorption mechanisms. Though these foot mechanisms can ensure robot stability on some occasions, it is difficult to be totally applied to the real-time acquisition of the ECA distribution especially for keeping balance on rough terrains. WS-1 (WASEDA Shoes-No. 1) foot system [13] with cam-type locking mechanisms can contact on the ground as four points while could not maintain the large-scare four-point contact on the uneven ground while its foot meets obstacles. Yang et al. [14] proposed a new flexible foot system with 12 degrees of freedom that can automatically adapt to the three dimensional terrain. However, it has a low real-time performance due to revolute joints.

This paper describes our research efforts aimed at the perception of the ECA distribution under the robot feet [15]. The FFSA system was designed by the conception

* Corresponding author. Tel./fax: +86 551 6559 1337.
E-mail address: bywu@iim.ac.cn (B. Wu).

0263-2241/$ - see front matter © 2013 Elsevier Ltd. All rights reserved.
http://dx.doi.org/10.1016/j.measurement.2013.03.027

derived from the biomechanical information of human foot while in walking motion. Firstly, the Structure configuration, data acquisition and ECA processing methods of the FFSA system elaborately described in Sections 2–4, respectively. Secondly, in Section 5, the feasibility and validity of FFSA system are experimentally tested in the integrated perceptual foot (IPF) system of humanoid robot platform BHR-2. Finally, the conclusions and future works are provided in Section 6.

2. The structure configuration of FFSA system

Wherever a human foot is generally divided into forefoot, mid-foot, and hind-foot, which represent the toes and frontal part, foot arch, and the heel, respectively. The foot–sole contact areas are affected by the structure of the foot as well as the placement of portions of the foot during walking or running. Fig. 1 shows the contact area mainly distribute on the rear foot and forefoot sole from heel-strike to toe-off during single support phase in human walking motion [16]. Most of the present day humanoid robot feet are non-anthropomorphic with solid plate as feet. So during static or flat foot walking, the robot feet would not necessarily show unique contact area distributions, but in the case of dynamic walking or stepping on rough terrains.

To real-timely obtain the ECA distribution in robot walking motion, the simplest measurement type of resistive force sensor arrays have been adopted in the FFSA system with the consideration for light foot weight, small mounting space and being build in-sole sensory system. The FFSA are piezoresistive elements made by screen-printing of piezoresistive ink on thin polymer film substrate. Fig. 2 shows two such layers on which the ink is printed in rows and columns are joined together by an adhesive. The intersection of the rows of one layer with the columns of another layer becomes a pressure sensing element. Its characteristic is that its conductance value increases together with the intensity of a force applied on an active area. Every sensing element behaves a resistor and the resistance is affected by the contact on these surfaces. As shown in Fig. 3, the resistance is inversely proportional to the applied force. The hysteretic characteristics indicate low measurement accuracy.

If R is the resistance and conductance is given by

$$g = 1/R \tag{1}$$

then the gauge factor g_f is given by

$$g_f = g/F \tag{2}$$

where F is the applied force.

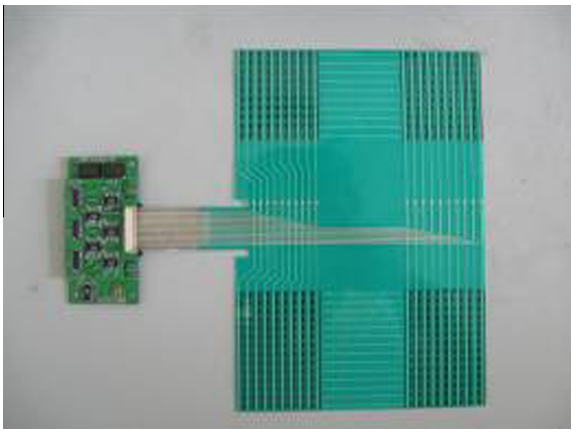

Fig. 2. The FFSA with spatial resolution 5 mm × 5 mm.

The FFSA have a geometry suited for contact area distribution measurement of foot sole contact on ground. Each sensor array element can be addressed by its corresponding row and column. The connections are populated arbitrarily according to requirements of foot contour, and hence the periphery of the sensor film can be trimmed into two parts for the fist-generation prototype shown in Fig. 4, the frontal part is 150 mm × 60 mm in dimension corresponding to the fore sole of human foot. The heel part is 150 mm × 40 mm to the rear sole, since it is flexible and very thin (0.22 mm) and well suited for in-sole measurements; the spatial resolution is 5 mm × 8 mm, and there are about 448 sensing elements.

The FFSA are attached between the lower surface of flat plate sole which is designed curvedly at two ends and the lower layer also called shock absorption layer which contact directly with ground. FFSA behave some switches, however conductance value changes rapidly after pressure reaches a threshold set in advance. It is not fit for accurate measurement because measurement value has an error rating of about F5–F25%. Nonetheless, we do not measure a force precisely, but we use it for measuring force distribution area by calculating the threshold of the loads applied to each FFSA. The FFSA system has only a bandwidth of about 100 Hz, which is lower than the response time for robot control system. So here we merely concern about the contact area rather than applied forces and get bandwidths up to about 200 Hz (*nearly* 5 ms).

Furthermore, the parts of FFSA adhere to the front arc surface and rear arc surface (shown in Fig. 5) can also serve as the switch at heel-strike and toe-off stance respectively for bionic gait planning generation.

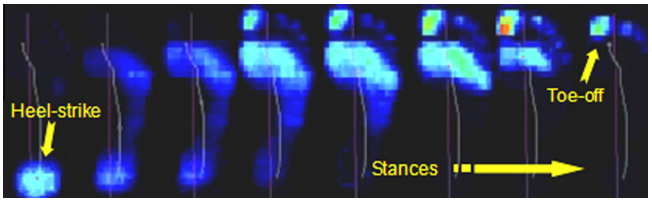

Fig. 1. The evolution of contact area distribution from heel-strike to toe-off stances in human walking.

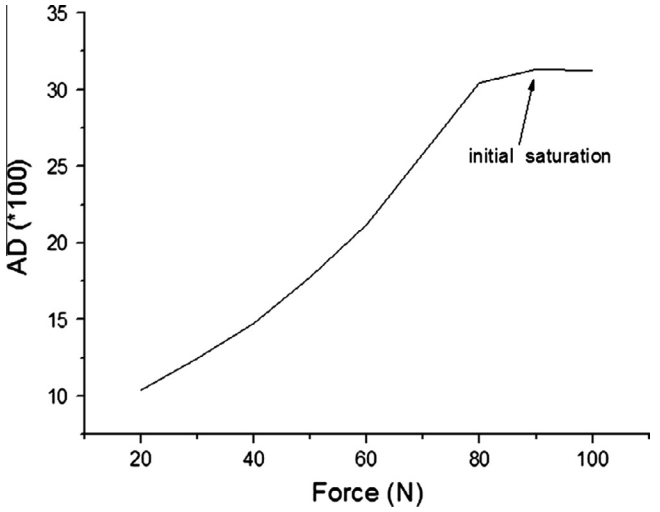

Fig. 3. The relationship between resistance of sensing element and applied force.

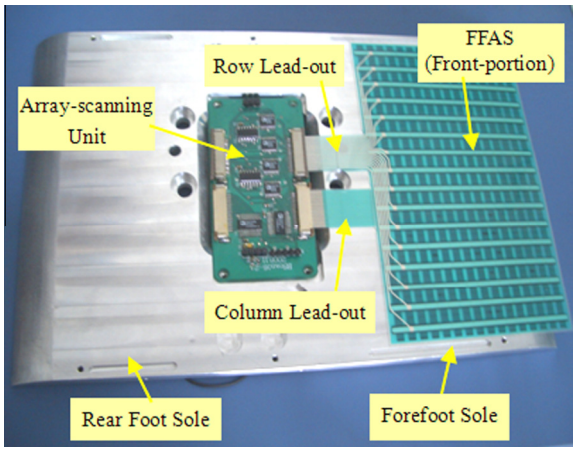

Fig. 4. The FFSA film trimmed to two portions are adhered to the forefoot sole plate and rear parts respectively with the scanning unit embed in the post-midst part of sole plate (here rear portion not shown).

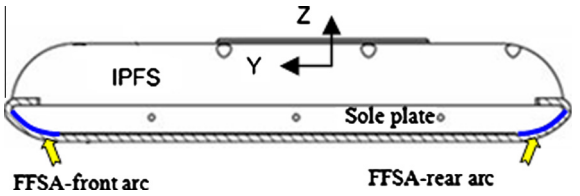

Fig. 5. FFSA at the front arc surface and rear arc surface are configured as switch to detect heel-strike and toe-off phase.

3. Data acquisition of FFSA system

The conductance value of the sensor element is directly proportional to the force applied on it. It is implied that a FFSA element lies in the effective supporting area when the value of force applied on it exceeds the force threshold value (*set in advance experimentally from* 2 to 10 kg). The sensing and scanning theory diagram based on the threshold setting.

As shown in Fig. 6, for scanning the resistors R_{ij} (the sensing element at the intersection of the row i with the *column* j), the output V_{ij} of FFSA can be obtained by controlling the multiplex switch and 2-way switch to i and V_{cc} respectively.

$$V_{ij} = \frac{R_0}{R_0 + R_{i(j-1)} || R_{ij} || R_{i(j+1)}} V_{cc} \tag{3}$$

where the symbol "||" denotes the resistance shunt in parallel. And then the 2-way switch to ground while other states remains unchanged, the output V_{ij} of FFSA can be expressed by:

$$V_{ij}^{-} = \frac{R_{ij} || R_0}{R_{ij} || R_0 + R_{i(j-1)} || R_{i(j+1)}} V_{cc} \tag{4}$$

From Eq. (5) and (6), the conductance value of R_{ij} can be educed by

$$g_{ij} = \frac{1}{R_0} \times \frac{V_{ij} - V_{ij}^{-}}{V_{cc} - V_{ij}} \tag{5}$$

The variable resistors R_{ij} represents the pressure sensing elements at the intersection of the rows i and the column j. The data of contact position and area between the foot and the ground can be synthetically operated by the centre processing system–DSP microprocessor and timely transmitted to the central control system of robot (CCSR) through the communication bus with a bandwidth of about 1000 Hz (shown in Fig. 7).

4. ECA processing method of FFSA system

4.1. Segmentation of force threshold

Every rectangular lattice represents a sensing array element and the black rectangular lattice shows contact force applied on it (as shown in Fig. 8a). The rectangular lattice (i, j), for example, represent the sensing array element lo-

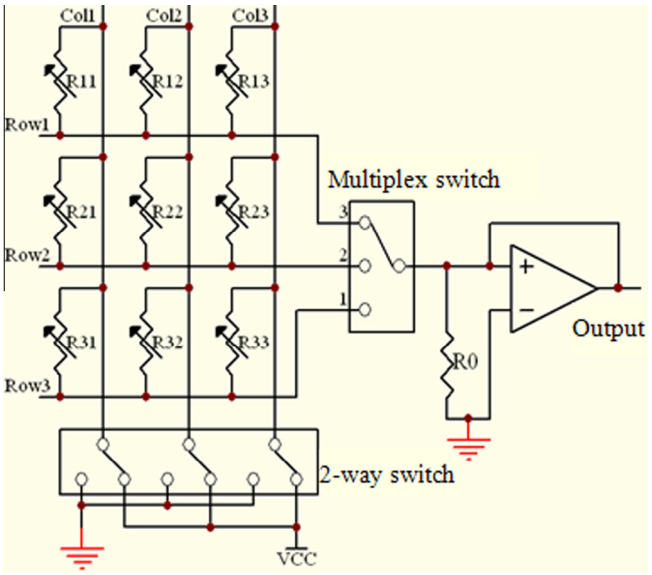

Fig. 6. Conceptual schematics of the FFSA system hardware with the multiplex switch to select the row and column.

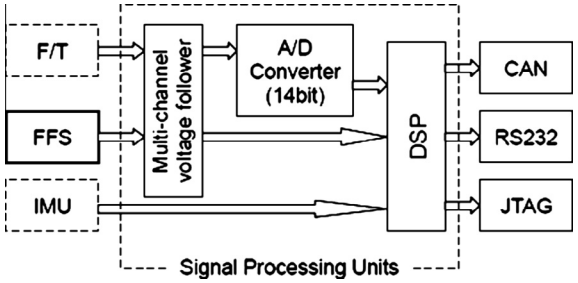

Fig. 7. The block diagram of the signal processing of the FFSA system in IPF system.

cated at the lattice intersection of the row i and the column j, where i denotes the row number of array elements ($1 \leqq i \leqq 8$), and j denotes the column number of array elements ($1 \leqq j \leqq 8$). F_{ij} denotes the force applied on the sensing array element at the rectangular lattice (i, j). The mean force values F_{ij} of all sensing array elements are sampled. The contact area formed by those sensing array elements whose force values are more than the force threshold F_{Th} value (*set in advance*) can be considered as the ECA.

4.2. Detection of support contour

After the processing of step (a), the maximum and the minimum coordinate of sensing array element in the row i are defined as MAX_i and MIN_i, respectively. It did not be disposed if there is only one or no sensing array element in a row. Thus we can extract the edge elements of the ECA (represented by those black rectangular lattices shown in Fig. 8b).

4.3. Reconstruction of ECA

The two elements MIN_i and MIN_{i+1} ($i = 1$–7) are connected to form the line $l^{\min}_{i\_i+1}$,

$$l^{\min}_{i\_i+1} \sim Y = \left|\frac{1}{MIN_{i+1} - MIN_i}\right| X = MX \tag{6}$$

If

$$\left|\frac{k-i}{MIN_k - MIN_{i+1}}\right| \geqslant M, (i+1 < k \leqslant 7) \tag{7}$$

The element MIN_{i+1} is right in the ECA, and then connect the two new elements MIN_{i+1} and MIN_{i+2} to form a new line $l^{\min}_{i+1\_i+2}$ repeatedly. If not, the two elements MIN_i and MIN_{i+2} are connected to form a new line $l^{+}_{i-(n+1)}$ to make judgment according to the processing procedure from Eq. (6) to Eq. (7) repeatedly until the sensing array element satisfying the condition defined by Eq. (7). And the processing procedure is just the same for MAX_i By the processing procedure, we can get the convex polygon area which forms the contour of ECA (*shown in* Fig. 9a).

4.4. ECA definition

The sensing array element satisfying the condition defined by Eq. (7) are connected in sequence to form contour of ECA which is shown in Fig. 9b.

5. Experiment on FFSA system

Practical tests about force applied on the FFSA system were performed by two convex parts in laboratory before mounted in the IPF system of robot to verify the display effect and the setting of force threshold value. Fig. 10 shows the test spot and the display effect of FFSA system.

The experiments on FFSA system located in the IPF system were conducted on the humanoid robot platform BHR-2. (The humanoid robot BHR-2 manufactured by the Intelligent Robotics Institute of Beijing Institute of Technology, China, is 160 cm tall and weighs approximately 51 kg. Its physical dimensions are based on anthro-

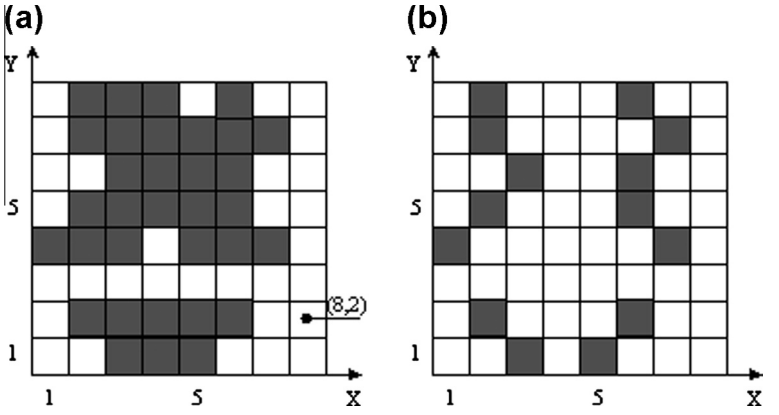

Fig. 8. (a) Segmentation result of applied force on sensing array elements, (b) Extraction of the edge elements of the ECA.

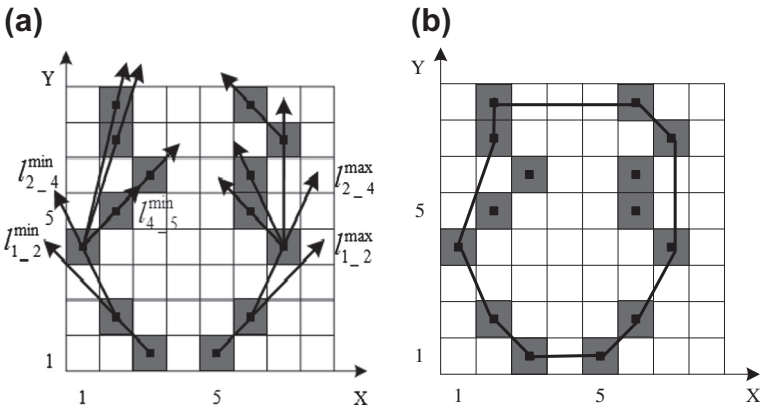

Fig. 9. (a) The contour of ECA formed by convex polygon area, (b) acquisition of ECA contour.

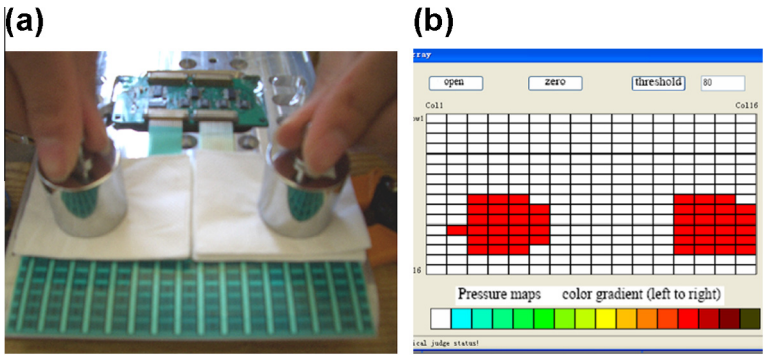

Fig. 10. (a) Laboratory tests on the FFSA system applied by two convex parts; (b) The ECA distribution obtained by the measurement system.

pometric data and have totally 32 degrees of freedoms (DoFs): the legs have six DoFs each, the pelvis has nine and the dead has two DoFs. BHR-2 can achieve stably bipedal walking based on pre-planning gait data). Fig. 11 shows the robot mounted the IPF system in ankles steps on a cable to estimate walking on uneven ground surface. The cable is arbitrarily about 5–10 mm in diameters as convex parts lying under the fore and rear part of the right sole plate. The ECA distribution can be obtained from the FFSA system and displayed by host computer software at a frequency of 1000 Hz (*shown in* Fig. 12). In dynamic and stable control of humanoid robot, the actual ECA lies in the peripheral contour that scanning points encompass rather than the contour of sole plate.

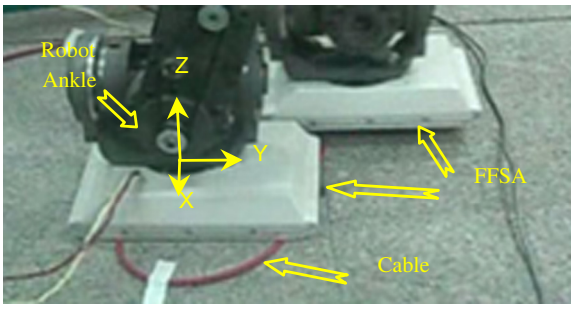

Fig. 11. The humanoid robot BHR-2 mounted with the FFSA system walks on uneven environment.

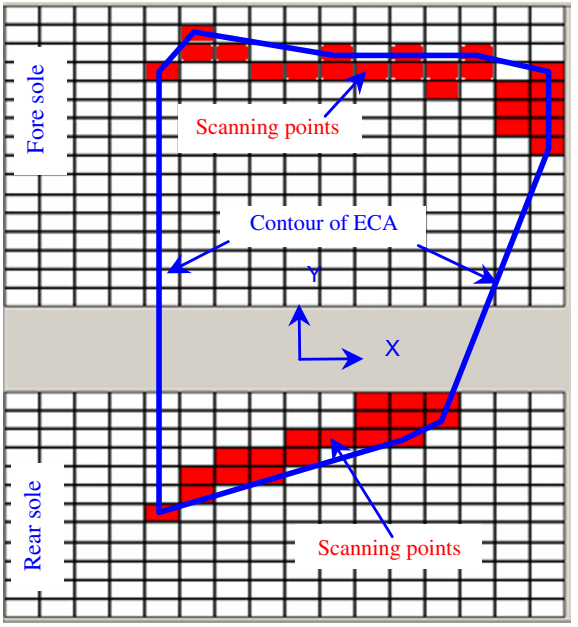

Fig. 12. ECA distribution on the foot sole measured by FFSA system.

6. Conclusions and future works

The FFSA system adopted in the IPF system of humanoid robot mainly concern the ECA distributions under the robot feet rather than the pressure distributions, thus giving higher scanning frequency. Reducing spatial resolution and effective perceptual elements would make the IPF system well suited for dynamic measurements and real-time control. However, in some degree it is difficult to detect the surface/terrain unevenness precisely with information from foot-sole pressure maps. So with the intelligent development of humanoid robot walking or running in human living spaces more anthropomorphically, the practical prospect of the FFSA system used in robot would become broad with the continuous perfection of fabrication process of sensor array film.

Additionally, an important point should be noticed that the sensor elements on the frontal arch and heel arc can detect the instant times of heel strike and toe off phase respectively, which is indispensable for bionic gait planning generation of humanoid robot. Our future work is to experiment on the real-time control of humanoid robot balance with information derived from the FFSA system.

Acknowledgments

This work presented in this paper was financially assisted by the National Project of High-tech and Research Program ("863" project) under Grant #2008AA04Z205; and the Anhui Provincial Natural Science Foundation under Grant #1308085MF86.

The authors give sincere thanks for the experiments research supports from the Laboratory of Bio-Robotics of Beijing Institute of Technology and the aid of technical assistance from the Research Center of Inf. & Tech. of Sports and Health, IIM, Hefei, China.

References

[1] Joel Chestnutt, Koichi Nishiwaki, James Kuffner, et al., An adaptive action model for legged navigation planning, Humanoids (2007) 196–202.
[2] Houman Dallali, Martin Brown, Bram Vanderborght, Using the torso to compensate for non-minimum phase behaviour in zmp bipedal walking, Adv. Rob. Res. 6 (2009) 191–202.
[3] Deok Hyeon Ko, Gyu Ro Kim, Soon Geul Lee, Stable walking algorithm using tilting motion for a bipedal robot: control of torso on 2-dimension plane of ZMP, in: International Conference on Control Automation and Systems, South Korea, 2010, pp. 1822–1825.
[4] Wu. Baoyuan, Jianfei Luo, Fei Shen, et al., Optimum design method of multi-axis force sensor integrated in humanoid robot foot system, Measurement 44 (2011) 1651–1660.
[5] Christine Chevallereau, Dalila Djoudi, Jessy W. Grizzle, et al., Stable bipedal walking with foot rotation through direct regulation of the zero moment point, IEEE Trans. Rob. 24 (2008) 390–401.
[6] K. Erbatur, O. Kurt, Natural ZMP trajectories for biped robot reference generation, IEEE Trans. Indus. Electron. 56 (2009) 835–845.
[7] J.P. Ferreira, M. Crisostomo, A.P. Coimbra, Human-like ZMP trajectory reference in sagittal plane for a biped robot, in: International Conference on Advanced Robotics, Portugal, 2009, pp. 1–6.
[8] K. Nishiwaki, S. Kagami, Strategies for adjusting the ZMP reference trajectory for maintaining balance in humanoid walking, in: IEEE International Conference on Robotics and Automation (ICRA), USA, 2010, pp. 4230–4236.
[9] M. Morisawa, F. Kanehiro, K. Kaneko, Reactive biped walking control for a collision of a swinging foot on uneven terrain, in: 11th IEEE-RAS International Conference on Humanoid Robots (Humanoids), Japan, 2011, pp. 768–773.
[10] Jun-Ho Oh, David Hanson, Won-Sup Kim, et al., Design of android type humanoid robot ALBERT HUBO, in: Proceedings of the IEEE/RSJ International Conference on Intelligent Robots and Systems, Beijing, China, 2006, pp. 1428–1433.
[11] Kenji Kaneko, Fumio Kanehiro, Shuuji Kajita, et al., Humanoid robot HRP-2, in: Proceedings of the IEEE International Conference on Robotics and Automation, New Orleans, IA, 2004, pp. 1083–1090.
[12] Masato Hirose, Kenichi Ogawa, Honda humanoid robots development, Philos. Trans. R. Soc. A 365 (2007) 11–19.
[13] K. Suwanratchatamanee, M. Matsumoto, S. Hashimoto, Haptic sensing foot system for humanoid robot and ground recognition with one-leg balance, IEEE Trans. Indus. Electron. Jpn. 58 (2011) 3174–3186.
[14] H. Yang, M. Shuai, Z. Qiu, et al., A novel design of flexible foot system for humanoid robot, in: IEEE Conference on Robotics, Automation and Mechatronics, China, 2008, pp. 824–828.
[15] Baoyuan Wu, Fei Shen, Yang Ren, et al., Development of an integrated perceptual foot system for humanoid robots, Rob. Auto. 27 (2012) 217–228.
[16] Chi-Wen Lung, Jen-Suh Chern, Lin-Fen Hsieh, et al., The differences in gait pattern between dancers and non-dancers, Mechanics 24 (2008) 267–273.